Solid State Sciences 12 (2010) 95–98

Contents lists available at ScienceDirect

Solid State Sciences

journal homepage: www.elsevier.com/locate/ssscie

Synthesis, crystal structure and optical properties of quasi-one-dimensional lead (II) iodide: $C_{14}H_{18}N_2Pb_2I_6$

K. Pradeesh [a], Monika Agarwal [b], K. Koteswara Rao [c], G. Vijaya Prakash [a,*]

[a] Nanophotonics lab, Department of Physics, Indian Institute of Technology Delhi, New Delhi-110016, India
[b] Department of Chemistry, Indian Institute of Technology Delhi, New Delhi-110016, India
[c] Department of Materials Science and Engineering, National Dong Hwa University, Hualien 974, Taiwan, ROC

ARTICLE INFO

Article history:
Received 17 June 2009
Received in revised form
25 September 2009
Accepted 14 October 2009
Available online 28 October 2009

Keywords:
Natural crystal growth
Inorganic–organic hybrid
Optical properties

ABSTRACT

Quasi-one-dimensional lead (II) iodide compound, $C_{14}H_{18}N_2Pb_2I_6$, with unique crystal structure was synthesized and solved for the crystal structure. These novel inorganic-organic hybrids have high thermal stability of upto 300 °C and show excitonic and charge-transfer features in their optical properties. An attempt has been made to understand the structural and optical mechanisms between inorganic one-dimensional polymeric PbI nano ribbons and the guest organic moiety for future applications in nanoscaled electronic devices.

1. Introduction

Self-assembly techniques take advantage of weak intermolecular interactions to create more complex crystal structures and preserve the unique characteristics of individual components. Current research is focused on synthesis of low-dimensional crystalline inorganic–organic metal halides with a possibility of incorporating properties associated with functional inorganic and organic moieties. Low-dimensional lead (II) iodide based hybrid crystals are of particular interest due to their unique structural, magnetic, optical nonlinear and optoelectronic functionality [1–9]. Due to the low-dimensionality, they show strong room-temperature excitonic optical features with large exciton binding energy and oscillator strengths. Apart from low-dimensionality, the large dielectric mismatch between the organic and inorganic moieties, greatly influences the physical and optical properties [10–12]. Low dimensional complexes include zero dimensional (0D), one dimensional (1D) and two dimensional (2D) lead iodide networks with organic moiety as spacers [8,10–15]. Among them, one-dimensional hybrids [16–21] are much attractive in nanoscaled electronic devices. Here the nature of organic moiety would modify overall inorganic–organic heterostructure arrangement and thereby the electronic interactions between inorganic 'nanowires' and organic moieties [22–24]. Here we report the synthesis, crystal structure, physical and optical features of quasi-one-dimensional compound, $C_{14}H_{18}N_2Pb_2I_6$. In this inorganic–organic hybrid the non-covalent interaction between organic and inorganic network unusually alter the normal coordination around Pb(II) and as a consequence the hybrid show unique optical and structural properties. These systems could also be visualized as inorganic polymeric 'nanoribbons' enclosed by organic spacers, in which the charger–transfer transition between the inorganic and organic moieties are of particular interest.

2. Experimental

Single crystals of Ethyl Viologen Lead Iodide ($C_{14}H_{18}N_2Pb_2I_6$) (hereafter EVPI), were grown by the slow evaporation technique. 0.1 mmol (23.05 mg) of lead (II) iodide was dissolved in 5 ml DMSO solution. Similarly 0.1 mmol (23.41 mg) of Ethyl Viologen diiodide ($C_{14}H_{18}N_2I_2$) (EVI) was dissolved in 5 ml of DMSO solution separately. The prepared solutions were mixed together at room temperature with constant stirring. The solution was allowed to evaporate slowly under controlled atmosphere. Within few weeks dark red single crystals of dimensions nearly $1 \times 0.2 \times 0.2$ mm^3 were grown. The crystals were filtered and dried for the single crystal X-ray diffraction studies. Single crystal diffraction studies were carried out by Bruker APEX CCD diffractometer with a Mo K_α

* Corresponding author. Tel.: +91 11 2659 1326; fax: +91 11 2658 1114.
E-mail address: prakash@physics.iitd.ac.in (G.V. Prakash).

1293-2558/$ – see front matter © 2009 Elsevier Masson SAS. All rights reserved.
doi:10.1016/j.solidstatesciences.2009.10.011

(0.71073 Å) sealed tube at 273 K. The program SMART [25] was used for collecting frames of data, indexing reflection and determination of lattice parameters, SAINT [25] for integration of the intensity of reflections and scaling. SADABS [26] was used for absorption correction and SHELXTL [27] for space group and structure determination and least-squares refinements on F^2. The lead atoms were located first and then remaining atoms were deduced from subsequent difference Fourier syntheses. The hydrogen atoms were located using geometrical constraints. All the non-hydrogen atoms were refined anisotropically. The least-squares refinement cycles on F^2 were performed until the model converged. Molecular graphics were presented by softwares, Mercury v2.2 and Diamond v2.1c.

Thermo-Gravimetry (TG) and Differential Thermo Gravimetry (DTG) were carried out between 30 and 800 °C at a scan rate of 5 °C/min under N_2 atmosphere.The crystals were dissolved in polar solvent, DMSO, and drop-coasted onto a glass substrate and was heated to about 65 °C. Once the solvent started evaporating, the substrate containing the solution has been quickly transferred to a spin-coater and spun at 1500 rpm for 30 s. The uniform dark red thinfilm thus obtained has been used for Glancing Angle X-ray Diffraction (GLAXRD) using CuKα radiation, UV–visible absorption and Photoluminescence (PL, excited at 330 nm) studies at room temperature. PL spectrum was acquired on Fluorolog-3 (FL 3–11) modular spectrofluorometer. PL imaging was carried out on modified FluoView (FV1000) laser scanning confocal microscope which was equipped with 447 nm excitation laser, rocking mirrors arrangement and a PMT.

3. Results and discussion

The compound crystallizes as monoclinic in the space group $P2_{1/c}$. The asymmetric unit consists of three $(PbI_3)^-$ units and one and a half molecule of ethyl viologen (EV^{2+}) units. The complete details of the crystallogaphic data are given in Table 1. The crystal structure features one-dimensional polymeric column of edge-shared PbI_6 octahedra. There are three types of iodide atoms defined by their connectivity. (a) Terminal atoms I(1), I(2) and I(11), (b) double bridging atoms I(3), I(4), I(5), I(6) and I(9) and (c) triple bridging iodide atom I(7). Similarly there are two types of lead atoms defined by their location within the column. (a) Outer lead atom Pb(1) bonded to terminal iodide and (b) inner lead atoms Pb(2) and Pb(3) bonded to triple bridging iodides.

Pb(1), Pb(2) and Pb(3) are collinear and are bonded to iodide atoms as shown in Fig. 1A. With the point of inversion C, at the middle of Pb(2), Pb'(2), I(4) and I′(4), all the atoms are repeated and are named with the primed ones. It is further to note that iodide atom I(10) is same as that of I(9) and I(8) is same as I(7). Including the centre of inversion symmetry, it forms a single unit and the column is extended by the edge sharing of iodide atoms I(5), I(7) and I(9) (Fig. 1C), extended along ⟨100⟩ direction. The shortest Pb–I distance (2.987(2) Å) is between Pb(1) to I(1) and Pb(1) to I(2) and the longest (3.394(2) Å) is between Pb(3) and I(11). The *cis* Pb–I bonding angles vary between 81.93(4)° and 95.44(7)°, while for *trans* Pb–I bonding angle varies between 179.61(5)° and 166.08(5)°, suggesting distorted PbI octahedra from its perfect structure. This could be due to the differences in the strengths of the covalent bonding between Pb atoms to the terminal, double bridging and triple bridging iodides. In one of the previously reported quasi-one-dimensional crystal [16], where the organic moiety is methyl-viologen (MV^{2+}), the PbI_6 octahedral structure is face-shared and MV^{2+} ions are accommodated in closely packed $[PbI_3]^-_\infty$ infinitely extended chains. However, in the titled compound three $(PbI_3)^-$ are edge-shared and repeated to form polymeric column, which is surrounded by organic moiety EV^{2+} di-cations in such a way to maximize the number of nearest neighboring iodine atoms around the cations (Fig. 1B). This is mainly due to the non-covalent interactions between inorganic and organic cation, for example, the nearest contact distance between N and I in the present case is 4.889 Å which is higher (3.629 Å) than that of the reported compound [16].

Table 1
Crystallographic data of ethyl viologen lead iodide ($C_{14}H_{18}N_2Pb_2I_6$).

Crystal data	Details
Empirical formula	$C_{14}H_{18}N_2Pb_2I_6$
Formula weight	2085.16 g/mol
a, Å	12.089(5)
b, Å	14.044(5)
c, Å	24.827(9)
Temperature	273(2) K
Radiation	MoK_α
Diffractometer	Bruker Smart Apex CCD
Crystal system	Monoclinic
Space group	$P2_{1/c}$
Volume	4215(3) Å^3
Z	4
d_{calc}, g cm^{-3}	3.286
Crystal	Rod, dark red
Crystal size, mm	0.15 × 0.13 × 0.12
Data collection	
No. measured reflections	41,507
No. unique reflection	7836
No. observed reflections ($I > 2\sigma I$)	4718
No. refined parameters	328
$R_1(I > 2\sigma I)$	0.0826
WR_2(all)	0.1587
Min/max $\Delta\rho$, ē Å^{-3}	−3.942/1.956

In organic cations, the values of individual C–C and C–N bond lengths range from 1.320(3) Å to 1.560(4)Å and 1.432(3)Å to 1.541(3) Å respectively. Within the hexagonal ring, the bond lengths of C–C and C–N varies from 1.270(3) Å to 1.280(3) Å having range of bond angles between 110.42(2)° and 126.38(2)°. Further, the inorganic–organic heterostructure is dominated by two kinds of hydrogen bonding between EV^{2+} di-cations to the PbI network: (1) terminal iodides and (2) nearby double bridging iodides with respective bond lengths 2.907 Å and 3.024 Å (Fig. 1). The complex heterostructure, therefore, affirms the importance of co-operative non-covalent bonding between organic and inorganic components.

Glancing Angle X-ray diffraction (GLAXRD) data suggest that prepared EVPI thinfilm are strongly oriented along ⟨011⟩ direction over the substrate (Fig. 2A). The Thermo-Gravimetry (TG) and Differential Thermo-Gravimetry (DTG) of EVPI (Fig. 2B)) suggest that they are quite stable up to 300 °C, higher than the values reported for other inorganic–organic hybrids [14,15,21]. Beyond 300 °C, the compound decomposes into PbI_2 with a weight loss of 32.8% (Fig. 2B). This weight loss is comparable to the calculated value (33.7%) obtained from the following decomposition process,

$$C_{14}H_{18}N_2Pb_2I_6(100\%) \rightarrow PbI_2(66.3\%) + C_{14}H_{16}N_2(15.3\%) + HI(18.4\%).$$

The optical absorption spectra of thin film shows a strong peak at 3.19 eV, associated with a broad shoulder at red end at ~2.8 eV (Fig. 3A). According to Ishihara et al. [12,22], the absorption peak at 3.19 eV could be attributed to the lowest excitons of PbI chains. The associated shoulder in the region of 2.4–2.8 eV is attributed to charge transfer (CT) transition between non-bonding state of the negatively charged PbI nanoribbons to the lowest unoccupied molecular orbital (LUMO) of the positively charged EV^{2+} di-cations.

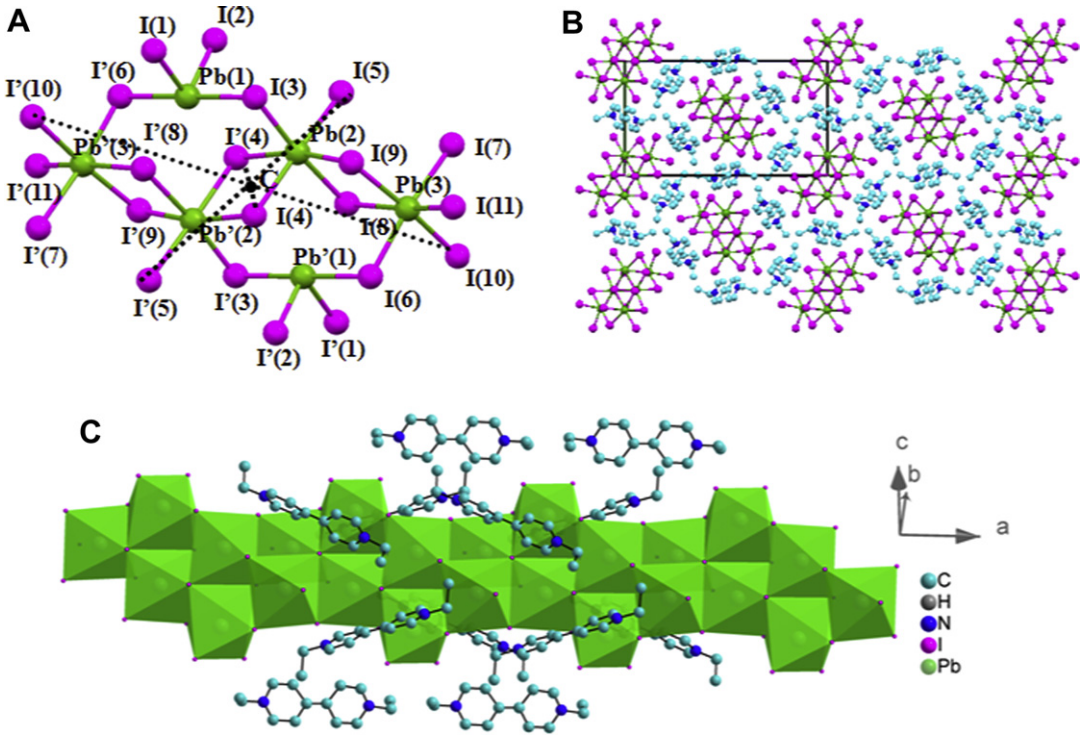

Fig. 1. (A) Structure formation of PbI column (B) Structure showing the unit-cell packing as viewed along 'a' direction. (C) The side view of the linear polymeric PbI column. All the hydrogen atoms of ethyl viologen molecules are omitted for clarity.

On the other hand, the photoluminescence spectra, of EVPI thin film show two distinct emission peaks: one at 2.35 eV associated with a shoulder at 2.19 eV and another intense peak at ~3 eV (Fig. 3A). The PL at 3 eV could be related to excitonic related transition. Other PL peak at 2.35 eV and the shoulder at 2.19 eV could be due to charge-transfer related transitions. However, it is to be noted that, unlike other 1D and 2D PbI based hybrids [15], EVPI is comparatively a poor emitter. For comparison, in those 1D and 2D Lead-based hybrids, optical bandgap of organic moiety (~6 eV) is much higher than inorganic (~3 eV), therefore the origin of PL is solely from low-lying inorganic exciton energy levels [28]. Whereas, in the present type of quasi- 1D crystals, such as methylviolegen lead iodide [12,29], organic (~4 eV) and inorganic (~3.4 eV) optical bandgaps are very close to each other. We have verified by performing extended Hückel tight-binding band structure calculation and found that the bandgap for the present molecule is 3.75 eV. Therefore, in these systems, charge-transfer transitions play a vital role rather than excitonic transitions. Apart from thin film emission, we have also recorded single crystal imaging using confocal high-resolution microscope, to confirm the morphology and emission characteristics. Fig. 3B reproduces the confocal (i) transmission (ii) laser scattering and (iii) Photoluminescence images. For laser scattering and PL imaging, crystals were excited with 447 nm (2.77 eV), 40 mW laser. A bandpass filter (BA465–495) has been used for PL measurements. In general, the absorption and emission transitions of EVPI thinfilms are distinctly red-shifted, compared to single crystal absorption and emission features of previously reported Methyl viologen lead iodide [12].

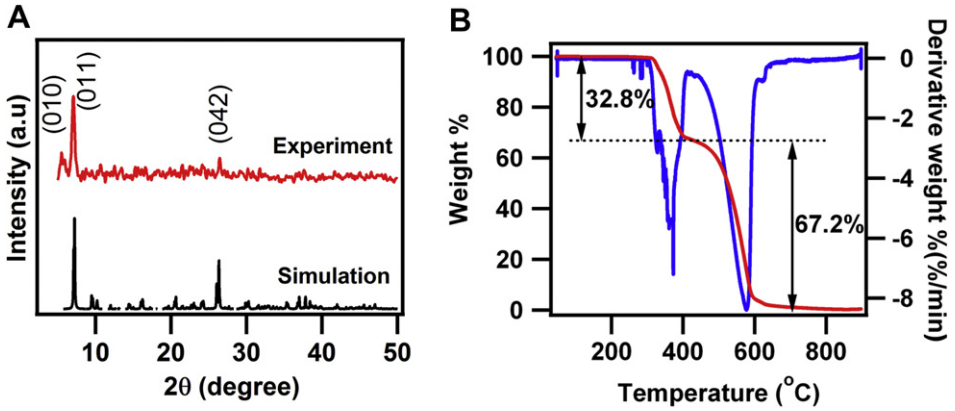

Fig. 2. (A) GLAXRD pattern of experimental EVPI thin film. Simulated powder pattern XRD from single crystal EVPI data is also shown for comparison. (B) Thermo-Gravimetry (TG) (red) and Differential Thermo-Gravimetry (DTG) (blue) curves of EVPI compound. Here the decomposition weight loss is estimated as 32.8%, which is comparable to the calculated loss of 33.7%. (For interpretation of the references to colour in this figure legend, the reader is referred to the web version of this article).

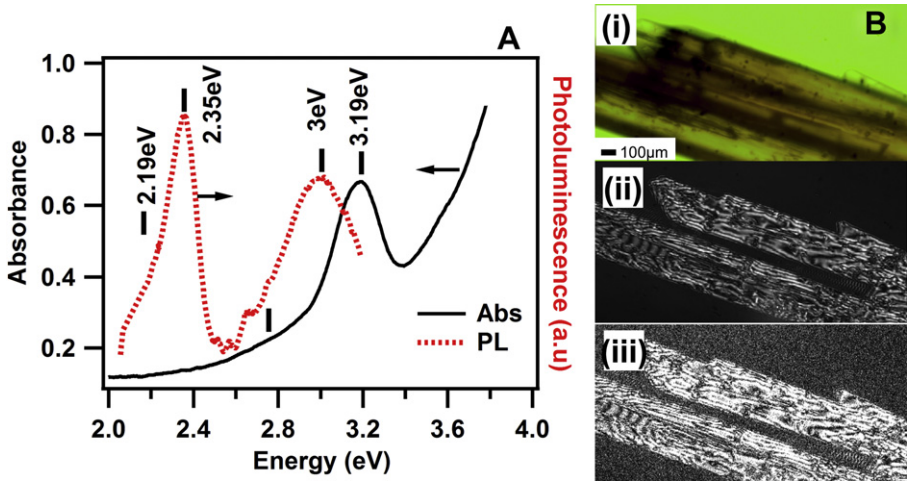

Fig. 3. (A) Absorption (black) and emission (red) spectra of EVPI thin film and (B) (i) Confocal, (ii) Laser Scattering and (iii) Photoluminescence (PL) images of EVPI crystals. (For interpretation of the references to colour in this figure legend, the reader is referred to the web version of this article).

In general, these compounds are of much importance, specially understanding the behavior of charge carriers in these quasi-one-dimensional systems for many electronic and optoelectronic applications. Experiments such as photo and electronic conductivity experiments are needed to understand electronic interactions between inorganic and organic molecules. Those experiments are currently under progress in our labs.

4. Conclusions

Here we have synthesized unique one-dimensional lead iodide polymeric nanoribbons: Ethyl viologen lead iodide (EVPI). Detailed crystal structure of EVPI was solved and analysed. The unusual crystal structure features one-dimensional column of edge-shared PbI_6 octahedra, where the non-covalent interaction between organic and inorganic moieties modifies the layered PbI_2 network into complex 1D polymeric column. The thermal stability of these one-dimensional crystals is as high as 300 °C. In thin film form, they are ordered in (011) direction and show distinct excitonic as well as strong charge-transfer related absorption and emission characteristics. These one-dimensional hybrids are of considerable attention in nanoscaled electronic devices; therefore, for future applications, more experiments are needed to understand the mechanism between inorganic polymeric column and the guest organic moiety.

Acknowledgements

Authors are thankful to Prof. A Ramanan, Department of Chemistry, IIT Delhi, and Prof. J.J. Baumberg, Cavendish Laboratory, University of Cambridge, UK, for their helpful discussions. One of the authors (GVP) acknowledges the financial support from DST, India. This work is part of *UK-India Education and Research Initiative* (UKIERI) programme.

Supplementary data

Crystallographic data for the structure reported in this paper have been deposited with the Cambridge Crystallographic Data Centre as supplementary publication no. CCDC-720062. Copies of the data can be obtained free of charge on application to CCDC, 12 Union Road, Cambridge CB2 1EZ, UK (Fax: +44 1223 336 033; e-mail: deposit@ccdc.cam.ac.uk).

References

[1] D.B. Mitzi, K. Chondroudis, C.R. Kagan, Ibm. J. Res. Dev. 45 (1) (2001) 29–45.
[2] D.M. Mitzi, J. Mater. Chem. 14 (2004) 2355–2365.
[3] T. Gebauer, G.Z. Schmid, Z. Anorg. Allg. Chem. 625 (1999) 1124–1128.
[4] M. Shimizu, J. Fujisawa, T. Ishihara, J. Lumin. 122–123 (2007) 485–487.
[5] A. Masui, K. Matsuishi, S. Onari, Phys. Status Sol. B. 223 (2001) 501–505.
[6] M. Shimizu, Phys. Rev. B 71 (2005) 033316.
[7] C. Symonds, J. Bellessa, J.C. Plenet, A. Bréhier, R. Parashkov, J.S. Lauret, E. Deleporte, Appl. Phys. Lett. 90 (2007) 091107.
[8] A.M. Guloy, Z. Tang, P.B. Miranda, V.I. Svdanov, Adv. Mater. 13 (2001) 833–837.
[9] A. Brehier, R. Parashkov, J.S. Lauret, E. Deleporte, Appl. Phys. Lett. 89 (2006) 171110.
[10] T. Ishihara, J. Takahashi, T. Goto, Phys. Rev. B 42 (1990) 11099–11107.
[11] X. Hong, T. Ishihara, A.V. Nurmikko, Phys. Rev. B 45 (1992) 6961–6964.
[12] J. Fujisawa, T. Ishihara, Phys. Rev. B 70 (2004) 113203.
[13] Y. Takeoka, K. Asai, M. Rikukawa, Kohei Sanui, Chem. Lett. 34 (2005) 602–603.
[14] Z.L. Xiao, H.Z. Chen, M.M. Shi, G. Wu, R.J. Zhou, Z.S. Yang, M. Wang, B.Z. Tang, Mater. Sci. Engineer. B 117 (2005) 313–316.
[15] G. Vijaya Prakash, K. Pradeesh, R. Ratnani, K. Saraswat, M.E. Light, J.J. Baumberg, J. Phys. D: Appl. Phys. 42 (2009) 185405.
[16] Z. Tang, A.M. Guloy, J. Am. Chem. Soc. 121 (1999) 452–453.
[17] V. Chakravarthy, A.M. Guloy, Chem. Commun. (1997) 697–698.
[18] T. Naito, T. Inabe, J. Solid State Chem. 176 (2003) 243–249.
[19] K. Tanaka, R. Ozawa, T. Umebayashi, K. Asai, K. Emac, T. Kondoa, Physica E 25 (2005) 378–383.
[20] G.A. Mousdis, V. Gionis, G.C. Papavassiliou, C.P. Raptopouloub, A. Terzisb, J. Mater. Chem. 8 (10) (1998) 2259–2262.
[21] N. Louvain, W. Bi, N. Mercier, J.Y. Buzare, C. Legeinc, G. Corbelc, Dalton Trans. (2007) 965–970.
[22] J. Fujisawa, N. Tajima, K. Tamaki, M. Shimomura, T. Ishihara, J. Phys. Chem. C 111 (2007) 1146–1149.
[23] N. Miyamoto, Y. Yamada, S. Koizumi, T. Nakato, Angew. Chem. Int. Ed. 46 (2007) 4123–4127.
[24] W. Bi, N. Leblanc, N. Mercier, P. Auban-Senzier, C. Pasquier, Chem. Mater. 21 (2009) 4099–4101.
[25] Smart & SAINT Software Reference Manuals, Version 6.22. Bruker AXS, Analytical Instrumentation, 2001, Madison, Wisconsin, USA.
[26] G.M. Sheldrick, SADABS, A Software for Empirical Absorption Correction. University of Gottingen, Gottingen, Germany, 2000.
[27] SHELXTL Reference Manual, Version 5.1. Bruker AXS, Analytical Instrumentation, 2000, Madison, Wisconsin, USA.
[28] T. Umebayashi, K. Asai K, T. Kondo, A. Nakao, Phys. Rev. B. 67 (2003) 155405.
[29] J. Fujisawa, N. Tajima, Phys. Rev. B. 72 (2005) 125201.